Direct evidence of band modification and suppression of superstructure in $TiSe_2$ upon Fe intercalation: An angle-resolved photoemission study

X. Y. Cui,[1] H. Negishi,[2] S. G. Titova,[3] K. Shimada,[4,*] A. Ohnishi,[5] M. Higashiguchi,[1] Y. Miura,[1] S. Hino,[5] A. M. Jahir,[5] A. Titov,[6] H. Bidadi,[7] S. Negishi,[4] H. Namatame,[4] M. Taniguchi,[4] and M. Sasaki[5]

[1]*Graduate School of Science, Hiroshima University, Kagamiyama 1-3-1, Higashi-Hiroshima 739-8526, Japan*

[2]*Graduate School of Advanced Sciences of Matter, Hiroshima University, Kagamiyama 1-3-1, Higashi-Hiroshima 739-8530, Japan*

[3]*Institute of Metallurgy, Urals Division of RAS, 620016 Yekaterinburg, Russia*

[4]*Hiroshima Synchrotron Radiation Center, Hiroshima University, Kagamiyama 2-313, Higashi-Hiroshima 739-0046, Japan*

[5]*Department of Physics, Faculty of Science, Yamagata University, Kojirakawa 1-4-12, Yamagata 990-8560, Japan*

[6]*Institute of Metal Physics, Urals Division of RAS, 620219 Yekaterinburg GSP-170, Russia*

[7]*Department of Physics, Faculty of Science, Tabriz University, Tabriz 51664, Iran*

(Received 26 October 2005; revised manuscript received 30 December 2005; published 16 February 2006)

We present electrical resistivity (ρ) measurements for the intercalation compound Fe_xTiSe_2 ($0 \leqslant x < 0.16$) over the temperature range from 4.2 to 300 K, and angle-resolved photoemission spectra for $x=0$, 0.05, and 0.14 at 50 and 250 K (or 280 K). At 250 K, $TiSe_2$ is a semimetal having hole pockets centered at the Γ point and electron pockets around the L points of the Brillouin zone. Upon intercalation, Fe-derived flat bands appear just below the Fermi energy, and the Se $4p$ derived bands forming hole pockets at the Γ point are lowered. At 50 K, band folding due to $2a \times 2a \times 2c$ superlattice is observed clearly near the L point for the host and $x=0.05$, while it vanishes for $x=0.14$, consistent with the ρ-T data. The critical concentration for the suppression of the superstructure ($0.05 < x_c \leqslant 0.075$) can be explained reasonably well by the percolation threshold of a two-dimensional-trianglar lattice consisting of seven Ti atoms, which is estimated to 1/14 (=0.0714).

DOI: 10.1103/PhysRevB.73.085111 PACS number(s): 71.20.−b, 79.60.−i, 71.70.−d

I. INTRODUCTION

Intercalation of $3d$ transition metals into the van der Waals (vdW) gaps of layered materials modifies structural, transport, and magnetic properties of the host materials, which makes it a candidate of a multifunctional material system controlled by the guest species and their concentration.[1–3] In order to understand the physical properties of such systems, it is indispensable to elucidate how the electronic-band structures, especially near the Fermi level (E_F) of the compounds, are modified by intercalation. Angle-resolved photoemission spectroscopy (ARPES) is a powerful method to examine occupied valence bands in solids.[4–7] In the present work, we report measurements of transport properties of Fe_xTiSe_2 ($0 \leqslant x < 0.16$) single crystals and ARPES results for three samples with $x=0$, 0.05, and 0.14. The host material $TiSe_2$ has a CdI_2-type layered structure ($a=3.536$ Å, $c=6.004$ Å) with the space group $P\bar{3}m1$ and a hexagonal first Brillouin zone (BZ), as depicted in Fig. 1(a). On the basis of the band-structure calculation,[8] $TiSe_2$ is a semimetal having an electron pocket at the L point derived from the Ti $3d_{z^2}$ states and hole pockets at the Γ point derived mainly from Se $4p$ states. The electrical resistivity (ρ) of $TiSe_2$ passes through a maximum when it is cooled below 200 K, which is associated with a $2a \times 2a \times 2c$ superlattice formation.[9] Although the transition has been discussed in terms of an excitonic insulator mechanism[10] or a band-type Jahn-Teller (JT) mechanism,[11] its origin has not been fully clarified yet.

The Fe atoms are inserted into the octahedral sites of the vdW gaps, and modify the electronic structure of $TiSe_2$. In this paper, we will show a clear semimetal-to-metal transition at $x \sim 0.07$ above which the anomalous resistivity behavior disappears. ARPES results clearly show that flat bands are formed near E_F and that Se $4p$ derived states around the Γ point are lowered upon Fe intercalation. Both effects are discussed in terms of the bond formations between the Fe-Se atoms and between Ti-Fe-Ti atoms. Furthermore, a band folding due to the $2a \times 2a \times 2c$ superlattice formation in $TiSe_2$[9,12] is suppressed by Fe intercalation; the effect is observed for $x=0.05$, and fully completed for $x=0.14$. The value of the critical concentration, x_c, of the destruction of the ordered phase will be discussed in terms of a percolation theory for a two-dimensional-triangular lattice.

II. EXPERIMENT

Fe_xTiSe_2 ($0 \leqslant x < 0.16$) single crystals used in the present study were grown by a chemical vapor transport technique

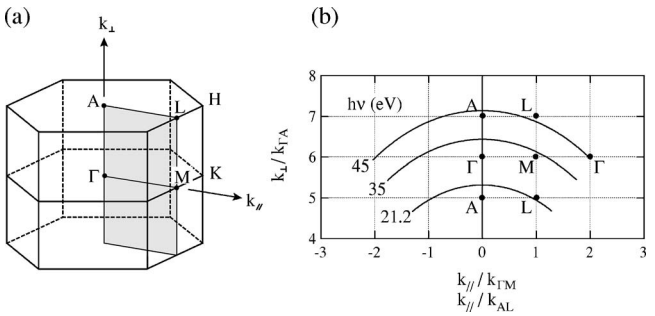

FIG. 1. (a) First Brillouin zone of the host $TiSe_2$ in the normal phase. (b) Contours in $k_\perp - k_\parallel$ plane at E_F by scanning polar angle $|\theta| \leqslant 40°$ in the ARPES experiment for $h\nu=21.2$, 35, and 45 eV.

with a temperature gradient of 500–600 °C and iodine as a transport agent.[9] The host material, $TiSe_2$ single crystals, was grown at 500 and 900 °C. The Fe concentration x was determined by a microprobe element analysis using the x-ray microanalyzer of an electron microscope, JEOL-733. Powder x-ray diffraction measurements show that the in-plane lattice constant, a, increases with x, while the interlayer lattice constant, c, decreases, as already reported.[12–14] This indicates that Fe intercalation acts on the host layers as a source of chemical uniaxial pressure along the c axis. The relative variation is proportional to x, $|\Delta a/a| \sim |\Delta c/c| \sim 0.03x$ for $x \leqslant 0.25$.[14] The values of the lattice constants of single crystal samples as a function of the Fe concentration are in a good accordance with literature data,[13] which confirms the Fe concentration obtained from the x-ray microanalyzer.

The resistivity measurements were performed for Fe_xTiSe_2 ($0 \leqslant x < 0.16$) over the temperature range from 4.2 to 300 K using a *dc* potentiometric method with a four-probe arrangement. The ARPES measurements were done for three representative samples with $x=0$, 0.05, and 0.14 on a linear undulator beamline BL-1 at Hiroshima Synchrotron Radiation Center (HSRC), Hiroshima University.[15] The details of the ARPES apparatus were reported elsewhere.[16] Single crystalline samples were mounted on a He-flow-type cryostat, and the sample temperature was set at 50 and 250 K (or 280 K). In order to obtain clean sample surfaces, we cleaved samples on the cryostat just before the experiments. Total energy resolution was set at 28 meV for $h\nu=21.2$, 35, and 45 eV, and angular resolution is $\Delta\theta=0.3^\circ$ ($\Delta k=0.011$ -0.017 Å^{-1}).

The parallel and perpendicular components of the photoelectron wave vector relative to the surface, $k_\parallel$ and $k_\perp$, were evaluated by the relations $k_\parallel=\sqrt{2mE_k/\hbar^2}\sin\theta$ and $k_\perp=\sqrt{2m(E_k\cos^2\theta+V_0)/\hbar^2}$, where V_0 stands for the inner potential, and E_k the kinetic energy of the photoelectron.[17] Here we assumed $V_0=13$ eV, on the basis of the results obtained by ARPES and of previous experiments.[18,19] Figure 1(b) shows contours in the $k_\perp - k_\parallel$ plane at E_F by scanning the polar angle $\theta \leqslant \pm 40^\circ$ in the ARPES experiment for $h\nu=21.2$, 35, and 45 eV.

III. RESULTS AND DISCUSSIONS

Figures 2(a)–2(c) show the temperature dependence of ρ (ρ-T curves) of Fe_xTiSe_2 ($0 \leqslant x < 0.16$). The host grown at 500 °C shows an anomalous behavior with a maximum at 170 K due to the $2a \times 2a \times 2c$ superlattice formation below the phase transition temperature $T_c=200$ K which is determined from the maximum in the $d\rho/dT$ vs T curve [Fig. 2(a)]. The transition temperature is in good agreement with the reported data for the nearly stoichiometric sample.[9] For the host grown at 900 °C, on the other hand, the peak in ρ is suppressed [dashed line in Fig. 2(a)], which is due to Ti self-intercalation. The decrease above T_c is attributed to a large softening of the zone-boundary L_1 phonon mode, as revealed by an x-ray thermal diffuse scattering study.[20]

For the low concentrations $0.01 \leqslant x \leqslant 0.05$, ρ-T curves show a small decrease and a minimum on cooling, and then an activationlike increase, followed by a metallic decrease or

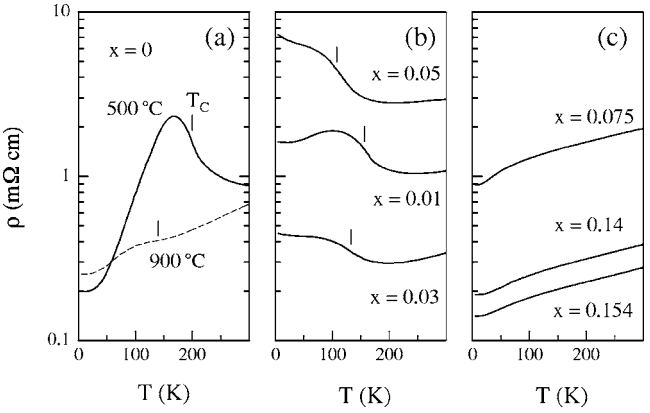

FIG. 2. The ρ-T curves for Fe_xTiSe_2 single crystals with (a) $x=0$, (b) $0.01 \leqslant x \leqslant 0.05$, and (c) $0.075 \leqslant x \leqslant 0.154$. The dashed line in (a) shows ρ for the samples grown at 900 °C. The bars show the characteristic transition temperatures T_c determined from the $d\rho/dT$-T curves.

a logarithmic increase [Fig. 2(b)]. These curves suggest that superlattice formation survives in this concentration range. As indicated by the bars in Figs. 2(a) and 2(b), T_c decreases with increasing x. On the other hand, the samples with higher Fe concentration $0.075 \leqslant x \leqslant 0.154$ show a metallic behavior and ρ decreases with x [Fig. 2(c)]. From these figures, we can see that the values of the electrical resistivity at 300 K show a maximum between $x=0.05$ and 0.075, and decrease for $x > 0.075$. The ρ-T curves indicate the existence of a critical concentration x_c ($0.05 < x_c < 0.075$) for the semimetal-to-metal transition. We shall discuss these transport results later in relation to the ARPES data.

Figure 3(a) shows the energy distribution curves (EDCs) of $TiSe_2$ at 250 K in the normal phase using $h\nu=45$ eV. In order to indicate energy bands clearly, we have taken the second derivative of the photoemission intensity along the energy direction. Figure 3(b) exhibits the intensity plot thus obtained, in a linear gray scale; the darker portion indicates the stronger spectral intensity, that is, where the energy bands are located.

The energy-band dispersion of $TiSe_2$ is similar to that of TiS_2 (Ref. 7), except for the details near E_F. At least two branches show maxima at the A point ($k_\parallel/k_{AL}=0$), minima at the L point ($k_\parallel/k_{AL}=\pm 1$), and they cross E_F at the Γ point ($k_\parallel/k_{AL}=k_\parallel/k_{\Gamma M}=2$). Thus, the valence top bands should have a dispersion along the ΓA direction, as well as along the in-plane (ΓM and AL) directions. A spectral feature with a small intensity is observed at the L point just below E_F, showing the existence of a small electron pocket, in agreement with previous works[18–21] and band-structure calculations.[8,22–24] Such a result is consistent with the experimental fact that the dominant carriers are holes in the normal states, as revealed by the Hall effect and the Seebeck effect measurements.[9]

Significant variations from the host band dispersion occur in the Fe intercalation compounds with $x=0.05$ and 0.14 [Figs. 4(a) and 4(c)]. Especially for the $x=0.05$ sample, one can clearly recognize more than four branches around the A point [Fig. 4(a)]. This indicates a modification of the Ti-Se

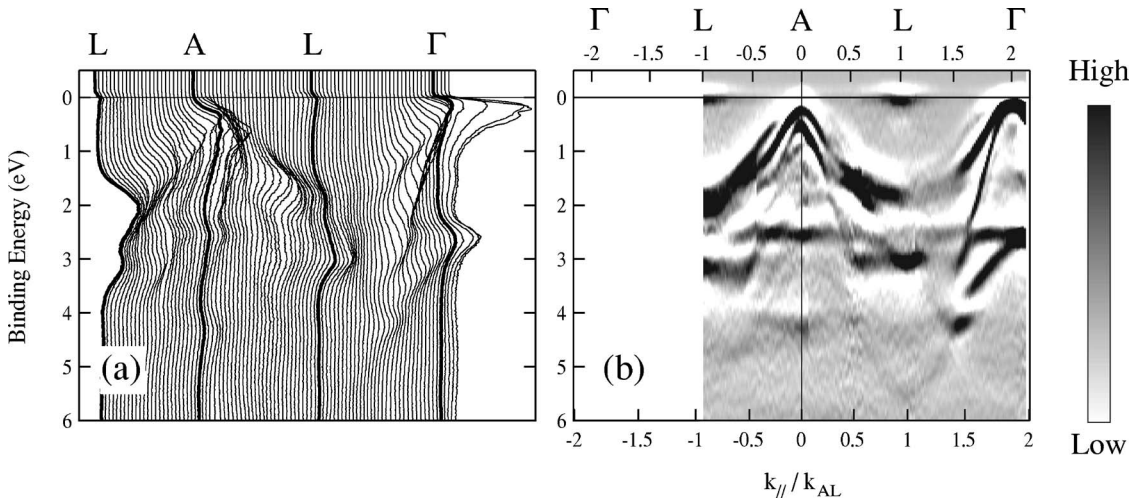

FIG. 3. ARPES result of $TiSe_2$ at 250 K using $h\nu$=45 eV. (a) EDCs, (b) intensity plot.

hybridization upon Fe intercalation. Figure 4(b) shows EDC around the A ($k_\parallel/k_{AL}$=0), L ($k_\parallel/k_{AL}$=1), and Γ ($k_\parallel/k_{AL}$=2) points. The intensity at the L point is increased indicating filling of the electron pocket.

The x=0.14 sample exhibits dispersive bands with a rather broad width at the A point [Fig. 4(c)]. The EDC for the L point in Fig. 4(d) shows a significant enhancement of spectral intensity compared with those for x=0 and x=0.05 samples. One can clearly see two flat bands at E_F and at the binding energy of ~0.3 eV in EDCs in Fig. 4(e). As the EDC for $k_\parallel/k_{AL}$=2 in Fig. 4(d) shows, the dispersive energy bands forming hole pockets near the Γ point are shifted away from E_F on Fe intercalation. Such a variation is strongly suggestive of a destruction of the periodicity along the c axis due to a random bridging of the layers by the intercalated Fe atoms. Since the band position is lowered at the Γ point, a charge transfers from Fe guest atoms to Ti and Se atoms to adjust their net valence states.

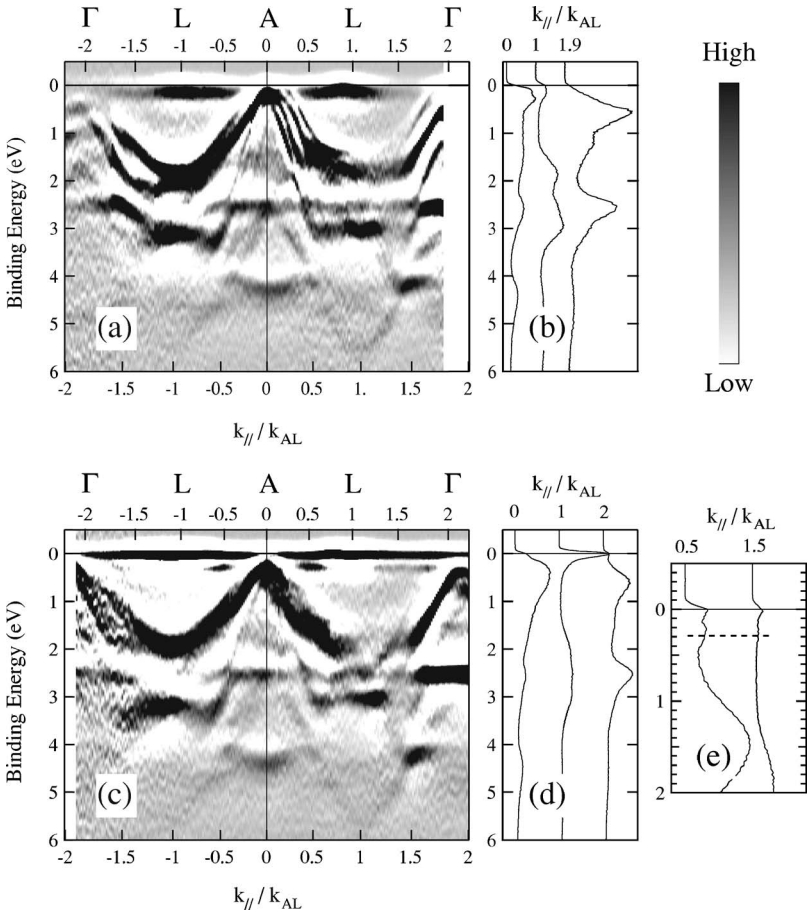

FIG. 4. ARPES results of Fe_xTiSe_2 (x=0.05 and 0.14) at 250 K using $h\nu$=45 eV. (a) The intensity plot for x=0.05. (b) EDCs at $k_\parallel/k_{AL}$=0, 1, 1.9, for x=0.05. (c) The intensity plot for x=0.14. (d) EDCs at $k_\parallel/k_{AL}$=0, 1, 2 for x=0.14. (e) EDCs at $k_\parallel/k_{AL}$=0.5, 1.5 for x=0.14.

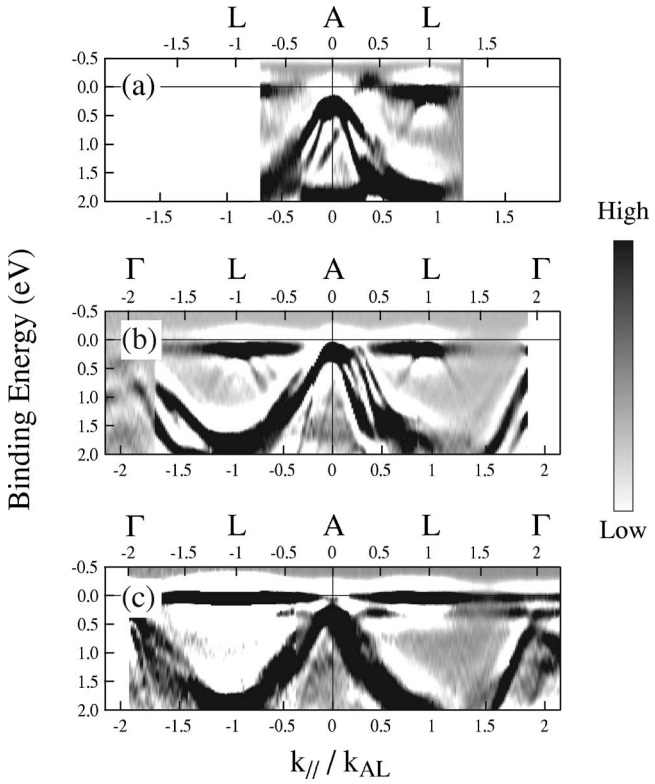

FIG. 5. The intensity plots near E_F of Fe_xTiSe_2 at 50 K; (a) $x=0$ at $h\nu=21.2$ eV, (b) $x=0.05$ at $h\nu=45$ eV, and (c) $x=0.14$ at $h\nu=45$ eV. Branches due to bandfolding appear around the L point for $x=0$ and 0.05.

The bond formation between Fe $3d_{z^2}$ and Ti $3d_{z^2}$ states should be responsible for the two flat bands for $x=0.14$, taking into account that similar flat bands also appear in Fe_xTiS_2 (Ref. 7) and $Fe_{0.25}TiTe_2$ (Ref. 25). The present results of Fe_xTiSe_2 is qualitatively consistent with theoretical results on $Fe_{0.25}TiS_2$,[26] in which net charges of the Ti, S sites, and Fe atom and charge transfer between Ti and Fe or between S and Fe are calculated by the full potential linear augmented plane-wave (FLAPW) method.

It is important to elucidate how Fe intercalation into the host material affects the $2a\times2a\times2c$ superlattice formation at low temperature. Figure 5(a) shows that branches appear at 50 K around the L point for $TiSe_2$. Note that a similar bandfolding is also clearly observed at the M point for $TiSe_2$ in Fig. 6(b). Above T_c the spectral intensity at the M point is very weak [Fig. 6(a)]. These observations are in agreement with the reported results for $TiSe_2$, and also with the $2a\times2a\times2c$ superlattice formation.[18,19,21] If the superlattice is realized, the volume of the Brillouin zone is $1/2\times1/2\times1/2=1/8$ of the original zone, and the L and M points become equivalent, as confirmed by the present results.

In Fig. 5(b), the $x=0.05$ sample clearly exhibits bandfolding at the L point. There is probably more than one branch, which is different from the $TiSe_2$ case. Instead of bandfolding, however, one can only see a flat band at the M point as Fig. 6(d) shows. The absence of bandfolding at the M point indicates that the superstructure formation along the c axis is inhibited by the Fe intercalation. The L and M points are no longer equivalent for $x=0.05$, which is a significant variation from the case of $TiSe_2$.

For the $x=0.14$ sample, no new signal of bandfolding at the L point has been observed at 50 K [Fig. 5(c)], besides clear flat bands at E_F and at 0.3 eV as in the higher temperature [Figs. 4(c)–4(e)]. The flat band is also clearly observed at the M point in Figs. 6(e) and 6(f). Thus, the bandfolding due to the superlattice formation was totally suppressed by the Fe intercalation at a concentration of $x=0.14$.

The destruction of the superlattice formation upon intercalation was already pointed out indirectly from the analysis of ρ-T data for substitution of Ti by other atoms such as Ta and V.[27] The critical concentration, x_c, is $0.05\sim0.075$ (Ref. 8), which is in agreement with the present result. Although the substitution of Se atoms by S atoms in $TiSe_{2(1-y)}S_{2y}$ also suppresses superlattice formation, the critical concentration is much higher, $y_c\sim0.5$ (Refs. 9 and 28). This value of y_c corresponds to the threshold concentration for site percolation on a two-dimensional-triangular lattice with a period constant a.[29]

In the following, we shall discuss the critical concentration of Fe_xTiSe_2, in relation to a percolation theory. According to the Monte Carlo simulation of the dichalcogenide layered host,[30] Fe guest atoms are distributed to avoid being on their nearest neighbor sites as a result from a repulsive interaction between guests. Then a guest Fe atom makes a strong bonding with six surrounding chalcogen atoms, while the bonding between Fe atoms are negligibly small because of the long inter-Fe distances in the case of $x<0.25$. Bonding between the Ti atoms above and below the Fe atom, Ti-Fe-Ti, takes place and it especially affects the electronic structure just near E_F, since the Ti $3d_{z^2}$ and Fe $3d_{z^2}$ states are the main contributors to the branches near E_F.

In order to understand the observed suppression of the $2a\times2a\times2c$ superlattice, however, we should pay attention to the remarkable displacements of the constituent Ti and Se atoms in the ordered states in the host, which are 0.08 and 0.02 Å, respectively, from the positions in the normal states,[9] as shown in Fig. 7(a). In earlier works,[9] a triple q mechanism for the charge-density wave (CDW) transition accompanying a $2a\times2a\times2c$ superlattice has been proposed, where the displacements of Ti atoms (open circles) and Se atoms (dots) shown in Fig. 7(a) results in the characteristic CDW temperature T_c. According to Whangbo and Canadell,[31] furthermore, the second-order JT effect is dominant for the superlattice formation in $TiSe_2$ rather than the first-order JT effect caused by the rotational deformation of Se atoms. An intercalated Fe atom forces to fix the surrounding Se atoms and next neighboring Ti atoms via the strong p-d hybridization [a Ti site over the intercalated Fe atom is represented by double open circles in Fig. 7(b)], inhibiting a large lattice distortion or a lattice softening to the vibration mode related to the superlattice formation. In other words, the intercalated Fe atom produces a cluster consisting of seven Ti atoms [Fig. 7(b)], which cannot participate with the host superlattice formation because of its large deformation energy. An additional cluster within a $2a$ distance must overlap by sharing one corner [Fig. 7(b)], while that separated by more than $\sqrt{7}a$ ($\sim2.65a$) cannot overlap. Therefore, we can suppose a cluster distribution on a two-dimensional triangular lattice of

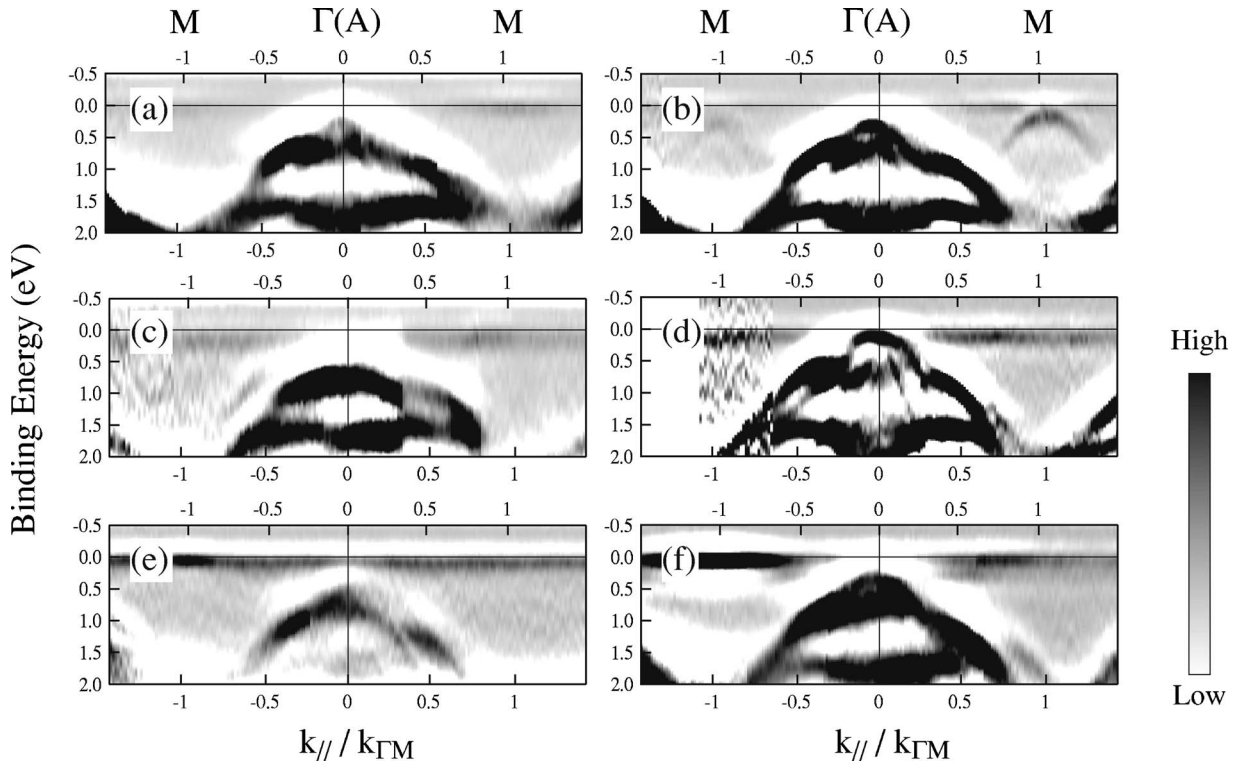

FIG. 6. Temperature variation in ARPES near E_F of Fe_xTiSe_2 at $h\nu=35$ eV. Left panels show results at high temperature; (a) $x=0$ (250 K), (c) $x=0.05$ (280 K), and (e) $x=0.14$ (250 K). Right panels show results at 50 K; (b) $x=0$, (d) $x=0.05$, and (f) $x=0.14$. Branches due to bandfolding appear around the M point for $x=0$, but are absent for $x=0.05$ and $x=0.14$.

$\sqrt{7}a\times\sqrt{7}a$ for Fe_xTiSe_2. Note that the two-dimensional lattice should be reasonable here since the superlattice formation along the c axis is suppressed by Fe intercalation for $x>0.05$ on the basis of the present ARPES results.

For a special Fe concentration of $x=1/7$, all sites of the lattice are occupied by clusters and there is no site to contribute to the host superstructure formation, as shown in Fig. 7(c). Then, the critical concentration x_c can be evaluated as a percolation threshold concentration on a two-dimensional-triangular lattice with a period constant of $\sqrt{7}a$, that is, $x_c=0.5(1/\sqrt{7})^2=1/14\sim0.0714$ (Ref. 29) which is in good agreement with the critical concentration for Fe_xTiSe_2 of $0.05<x_c\leqslant0.075$. Below x_c, the seven Ti atom clusters no longer percolate [Fig. 7(d)] and the network of superlattice can extend to the whole specimen; the superlattice can survive and influence physical properties. The concentration dependence of the electrical resistivity at 300 K, in which a maximum appears at $x_c=0.05\sim0.075$, and an increase of iron content leads to the resistivity drop [Figs. 2(b) and 2(c)], can be attributed to the fact that randomness is reduced above the threshold concentration.

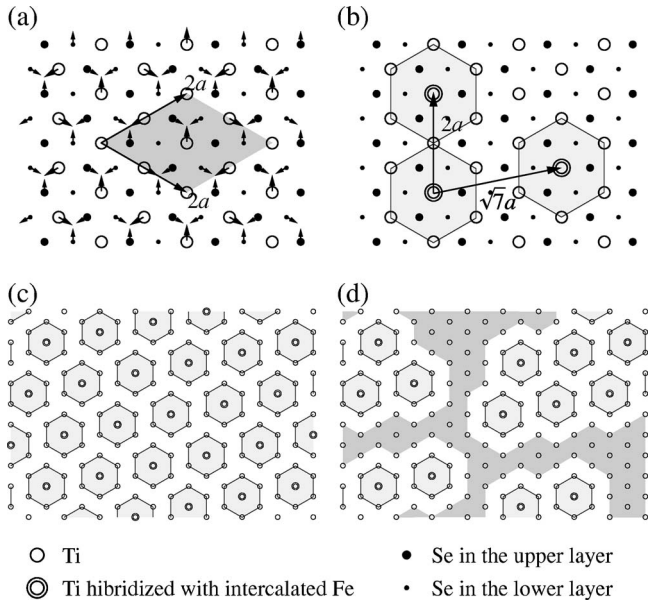

FIG. 7. Schematic diagrams of (a) displacements of Ti and Se atoms due to $2a\times2a$ superlattice formation in $TiSe_2$ and (b) a cluster consisting of seven Ti atoms caused by an Fe guest atom, where Ti and Se atoms are no longer displaced, as in the host. An additional cluster within $2a$ must overlap partially while another one separated by more than $\sqrt{7}a$ does not. Cluster distribution on a two-dimensional-triangular lattice of $\sqrt{7}a\times\sqrt{7}a$ for Fe_xTiSe_2 with (c) $x=1/7$ and (d) $x\sim1/14$, which correspond to a fully occupied state and a critical state of percolation threshold, respectively. Se atoms are omitted for simplicity.

IV. CONCLUSION

We have examined ρ-T curves and ARPES spectra of Fe_xTiSe_2 single crystal. The ρ-T curves indicates the semimetal-to-metal transition occurs at $0.05<x_c\leqslant0.075$. ARPES results indicated that flat bands appear near E_F, and

the Se $4p$ derived bands around the Γ point are lowered upon Fe intercalation. The bandfolding due to the $2a\times 2a\times 2c$ superlattice formation disappears above the critical concentration $x_c > 0.05$. This value of x_c can be well explained by the percolation theory of the cluster consisting of seven Ti atoms induced by the Fe intercalation. The percolation threshold for a two-dimensional-triangular lattice with a period constant of $\sqrt{7}a$ has been evaluated to be $x_c = 1/14 \sim 0.074$, which is in good agreement with the present experiments.

ACKNOWLEDGMENTS

This work was partly supported by a Grant-in-Aid for Scientific Research (No. 17654060) and for COE Research (13CE2002) of the Ministry of Education, Culture, Sports, Science and Technology of Japan, and by Russian Foundation for Basic Research (Grant Nos. 05-03-32200 and 05-03-32207). We thank the Materials Science Center, N-BARD, Hiroshima University for supplying liquid helium. The synchrotron radiation experiments have been done under the approval of HSRC (Proposal No. 04-A-50).

*Corresponding author. Email address: kshimada@hiroshima-u.ac.jp

[1] M. Inoue, H. P. Hughes, and A. D. Yoffe, Adv. Phys. **38**, 565 (1989).

[2] *Recent Advances in Magnetism of Transition Metal Compounds*, edited by A. Kotani and N. Suzuki (World Scientific, Singapore, 1993).

[3] N. V. Baranov, K. Inoue, V. I. Maksimov, A. S. Ovchinnikov, V. G. Pleschov, A. Podlensnyak, A. N. Titov, and N. V. Toporova, J. Phys.: Condens. Matter **16**, 9243 (2004) and references therein.

[4] Z.- X. Shen and D. S. Dessau, Phys. Rep. **253**, 1 (1995).

[5] M. Bovet, D. Popovic, F. Clerc, C. Koitzsch, U. Probst, E. Bucher, H. Berger, D. Naumovic, and P. Aebi, Phys. Rev. B **69**, 125117 (2004).

[6] T. Matsushita, S. Suga, A. Kimura, H. Negishi, and M. Inoue, Phys. Rev. B **60**, 1678 (1999).

[7] S. Suga, Mol. Cryst. Liq. Cryst. Sci. Technol., Sect. A **341**, 9 (2000).

[8] For review, K. Motizuki and N. Suzuki, *Microscopic Theory of Structural Phase Transitions in Layered Transition-Metal Compounds*, edited by K. Motizuki (Dortrecht-Reidel, Berlin, 1986).

[9] F. J. DiSalvo, D. E. Moncton, and J. V. Waszczak, Phys. Rev. B **14**, 4321 (1976).

[10] J. A. Wilson, Solid State Commun. **22**, 551 (1977).

[11] H. P. Hughes, J. Phys. C **10**, L319 (1977).

[12] A. V. Kuranov, V. G. Pleshchev, A. N. Titov, N. V. Baranov, and L. S. Krasavin, Phys. Solid State **42**, 2089 (2000).

[13] Y. Arnaud, M. Chevreton, A. Ahouanjinou, M. Danot, and J. Rouxel, J. Solid State Chem. **17**, 9 (1976).

[14] A. N. Titov, Yu. M. Yarmoschenko, M. Neumann, V. G. Pleshchev, and S. G. Titova, Phys. Solid State **46**, 1681 (2004).

[15] K. Shimada, M. Arita, T. Matsui, K. Goto, S. Qiao, K. Yoshida, M. Taniguchi, H. Namatame, T. Sekitani, K. Tanaka, H. Yoshida, K. Shirasawa, N. Smolyakov, and A. Hiraya, Nucl. Instrum. Methods Phys. Res. A **467-468**, 504 (2001).

[16] K. Shimada, M. Arita, Y. Takeda, H. Namatame, K. Kobayashi, T. Narimura, H. Namatame, and M. Taniguchi, Surf. Rev. Lett. **9**, 529 (2002).

[17] S. Hüfner, *Photoelectron Spectroscopy*, 3rd ed. (Springer-Verlag, Berlin, 2003).

[18] T. E. Kidd, T. Miller, M. Y. Chou, and T.- C. Chiang, Phys. Rev. Lett. **88**, 226402 (2002).

[19] K. Rossnagel, L. Kipp, and M. Skibowski, Phys. Rev. B **65**, 235101 (2002).

[20] M. Holt, P. Zschack, H. Hong, M. Y. Chou, and T.- C. Chiang, Phys. Rev. Lett. **86**, 3799 (2001).

[21] Th. Pillo, J. Hayoz, H. Berger, F. Levy, L. Schlapbach, and P. Aebi, Phys. Rev. B **61**, 16213 (2000).

[22] A. Zunger and A. J. Freeman, Phys. Rev. B **17**, 1839 (1978).

[23] A. Leventi-Peetz, E. E. Krasovskii, and W. Schattke, Phys. Rev. B **51**, 17965 (1995).

[24] C. M. Fang, R. A. de Groot, and C. Haas, Phys. Rev. B **56**, 4455 (1997).

[25] K. Yamazaki, K. Shimada, H. Negishi, F. Xu, A. Ino, M. Higashiguchi, H. Namatame, M. Tanniguchi, M. Sasaki, S. G. Titova, A. Totov, and Y. M. Yarmoshenko, Physica B **351**, 262 (2004).

[26] H. Martinez, Y. Tison, I. Baraille, M. Loudet, and D. Gonbeau, J. Electron Spectrosc. Relat. Phenom. **125**, 181 (2002).

[27] F. J. DiSalvo and J. V. Waszczak, Phys. Rev. B **17**, 3801 (1978).

[28] J.- M. Lopez-Castillo, A. Amara, S. Jandl, J.- P. Jay-Gerin, C. Ayache, and M. J. Aubin, Phys. Rev. B **36**, 4249 (1987).

[29] For example, R. Zallen, *The Physics of Amorphous Solids* (John Wiley and Sons, New York, 1983).

[30] S. Negishi, H. Negishi, M. Sasaki, and M. Inoue, J. Phys. Soc. Jpn. **69**, 2514 (2000).

[31] M. H. Whangbo and E. Canadell, J. Am. Chem. Soc. **114**, 9587 (1992).